75th International Astronautical Congress (IAC), Milan, Italy, 14-18 October 2024.

IAC-24,A3,IP,34,x90442

Design and cases studies of CORTO, an open access rendering tool for celestial and artificial bodies

Mattia Pugliatti[a,*], Carmine Buonagura[b], Dario Pisanti[c], Niccolò Faraco[d], Andrea Pizzetti[e], Michele Maestrini[f], Francesco Topputo[g]

[a,*] *PostDoc, University of Colorado, 80303 Boulder, United States of America,* mattia.pugliatti@colorado.edu
[b] *PhD Student, Politecnico di Milano, 20156 Milan, Italy,* carmine.buonagura@polimi.it
[c] *PhD Student, Scuola Superiore Meridionale, 80138 Naples, Italy,* dario.pisanti@unina.it
[d] *PhD Student, Politecnico di Milano, 20156 Milan, Italy,* niccolo.faraco@polimi.it
[e] *PhD Student, Politecnico di Milano, 20156 Milan, Italy,* andrea.pizzetti@polimi.it
[f] *Assistant Professor, Politecnico di Milano, 20156 Milan, Italy,* michele.maestrini@polimi.it
[g] *Full professor, Politecnico di Milano, 20156 Milan, Italy,* francesco.topputo@polimi.it

[*] Corresponding author

Abstract

CORTO stands for Celestial Object Rendering TOol and is an open-source Python repository designed to address the limited availability of high-quality image-label pairs for space exploration. Leveraging Blender's capabilities, CORTO enables the synthetic generation of large, annotated datasets to support computer vision tasks, providing a flexible and modular solution that simplifies the creation of training data for data-driven algorithms and testing of traditional image processing methods. The tool is especially relevant for optical navigation tasks that require complex interdisciplinary pipelines. The paper highlights the tool's architecture and demonstrates its application in various scenarios, including missions to small bodies, the Moon, other planetary bodies, and around uncooperative man-made objects. With its modularity, CORTO supports external contributions and future enhancements to expand its coverage to additional scenarios.

Keywords: Rendering, Dataset generation, Synthetic images, Image processing.

1. Introduction

Access to high-quality image-label pairs is fundamental both for data-driven algorithms and for traditional image-processing methods. Unfortunately, due to the limited number of celestial bodies that have been imaged throughout the history of space exploration and due to geometric and illumination constraints that are intrinsic to the existing datasets from previously flown missions, the availability of high-quality data is limited. This adversely impacts the capability to create and train data-driven algorithms and to perform robust statistical characterization of traditional image processing pipelines.

Synthetic renderings offer a powerful alternative to generating large amounts of annotated images. To accomplish this and other tasks, this work presents an overview of the Celestial Objects Rendering TOol (CORTO), an open-access, object-oriented, Python repository that exploits Blender's functionalities to synthetically generate large, annotated datasets to be used for computer vision tasks.

CORTO has been designed with modularity and accessibility as its core strengths. These should foster collaboration between researchers in the development of a reliable, simple-to-use image-label pairs generator. The ultimate goal of CORTO is to remove the complexity of dataset generation and allow image processing designers to focus primarily on pipeline design and testing. This is particularly relevant for optical navigation tasks, which require challenging and interdisciplinary pipelines that elaborate image content into relative pose solutions. While the tool currently covers a range of celestial body scenarios, focused on minor bodies, the Moon, planetary bodies, and artificial bodies, future enhancements could broaden its capabilities to encompass additional environments.

Lastly, in the past decade there has been a proliferation of different useful tools for the generation of synthetic datasets:

- PANGU[1, 2, 3] stands for Planetary Planet and Asteroid Natural scene Generation Utility and is considered the state-of-the-art for rendering celestial bodies. It is a tool with robust, long-lasting, and documented development designed by the University of Dundee for the ESA. PANGU supports various advanced functionalities and is extensively used as the industry standard for ESA projects involving visual-based navigation algorithms. However, access to the software is regulated via licenses and often requires direct involvement with an ESA project.

- SurRender[4, 5] is proprietary software by Airbus Defense and Space[1] that has been successfully used in designing and validating various vision-based applications for space missions in which the company is involved. The software can handle objects such as planets, asteroids, stars, satellites, and spacecraft. It provides detailed models of sensors (cameras, LiDAR) with validated radiometric and geometric models (global or rolling shutter, pupil size, gains, variable point spread functions, noises, etc.). The renderings are based on real-time image generation in OpenGL or raytracing for real-time testing of onboard software. Surface properties are tailored with user-specified reflectance models (BRDF), textures, and normal maps. The addition of procedural details such as fractal albedos, multi-scale elevation structures, 3D models, and distributions of craters and boulders are also supported.

- SISPO[6] stands for Space Imaging Simulator for Proximity Operations and is an open-access image generation tool developed by a group of researchers from the universities of Tartu and Aalto, specifically designed to support a proposed multi-asteroid tour mission [7] and the ESA's Comet Interceptor mission [8]. SISPO can obtain photo-realistic images of minor bodies and planetary surfaces using Blender[2] Cycles and OpenGL[3] as rendering engines. Additionally, advanced scattering functions written in OSL are made available [4] that can be used in the shading tab in Blender to model surface reflectance, greatly enhancing the output quality.

- Vizard [5] is a Unity-based visualization tool capable of displaying the simulation output of the Basilisk[9] software[6]. Its main purpose is to visualize the state of the spacecraft, however, it has also been used for optical navigation assessment around Mars [10, 11, 12] and can simulate both terrestrial and small body scenarios [13].

- The simulation tools illustrated in [14, 15], that implements high-fidelity regolith-specific reflectance models using Blender and Unreal Engine 5[7]. The tools can render high-fidelity imagery for close proximity applications, particularly about small bodies, focusing on the high-fidelity simulation of boulder fields over their surfaces.

- AstroSym[16], developed in Python to provide a source of images for closed-loop simulation for GNC systems for landing and close-proximity operations around asteroids.

- SPyRender[17], also developed in Python, is used to generate high-fidelity images of the comet 67P for training data-driven IP methods for navigation applications.

- [18] have explored the simulation of icy moon surfaces like those of Enceladus and Europa to support stereo depth estimation for sampling autonomy [8].

- DEMkit and LunaRay [19] are a suite of applications used in the generation, analysis, and verification of terrain data and photometrically accurate renderings of the lunar surface.

Such efforts highlight the importance of synthetic image generators and underscore a wide range of scenarios that can be simulated with this approach. Ultimately, CORTO can be used both as a simple-to-use black box to handle dataset generation with the existing functionalities or be further developed for specific scenarios and applications. This is actively promoted by the tool's modularity, which encourages external contributions, and its public availability at `https://github.com/MattiaPugliatti/corto`.

Previous works in the literature have illustrated the rendering and post-processing capabilities [20] and procedural small-body generation capabilities [21]. In this work, CORTO's architecture and functionality are highlighted considering new application scenarios and a consolidated software architecture. First, in Section 2. the software architecture is presented, followed in Section 3. by a description of past and present case studies in which CORTO has been used. In Section 4.a walkthrough of the tutorials is presented. In Section 5.the tool validation with the Moon is illustrated, while final remarks are presented in Section 6.

2. Software architecture

CORTO architectures have been designed to be modular, simple to use, and to facilitate contributions from different developers. The current software version is 1.0,

[1] `https://www.airbus.com/en/products-services/space/customer-services/surrendersoftware`, last accessed 10th of September, 2024.

[2] `https://www.blender.org/`, last accessed 10th of September, 2024.

[3] `https://www.opengl.org/`, last accessed 10th of September, 2024.

[4] `https://bitbucket.org/mariofpalos/asteroid-image-generator/wiki/Home`, last accessed 10th of September, 2024.

[5] `https://hanspeterschaub.info/basilisk/Vizard/Vizard.html#`, last accessed 10th of September, 2024.

[6] `https://hanspeterschaub.info/basilisk/`, last accessed 10th of September, 2024.

[7] `https://www.unrealengine.com/en-US`, last accessed 10th of September, 2024.

[8] `https://github.com/nasa-jpl/guiss`

which reflects the minimum working architecture on top of which future capabilities will be built. An overview of the CORTO architecture is illustrated in Figure 1, which represents the different classes and their dependencies.

Starting from the *State* class, different settings, shape models, texture images, and parameters are loaded and saved as cortopy objects. A scene is defined by the interaction of 4 different classes: *Body*, *Camera*, *Sun*, and *Rendering*. In the case of multiple bodies and/or cameras, multiple objects can be instantiated. These 4 classes interact with each other in the *Environment* class. Lastly, the *Shading* and *Compositing* classes are similarly used to easily build up via code the node trees to be used in the shading and compositing tabs in Blender.

3. Case studies

CORTO has been extensively used for generating datasets and designing and validating image processing and visual-based GNC systems in various projects and missions.

Two notable CubeSat missions, Milani and LUMIO, have utilized CORTO for testing image processing algorithms. For the Milani Hera CubeSat [22], a 6U CubeSat scheduled to visit the Didymos binary system in 2027, CORTO was extensively employed in designing data-driven algorithms for image processing, testing object recognition algorithms, and validating visual-based applications within the CubeSat GNC subsystem.

In contrast, CORTO was used for testing the limb-based navigation algorithm for the LUMIO mission [23]. LUMIO is a 12U CubeSat that will orbit in a Halo orbit around the Earth–Moon L2 point as part of an ASI/ESA mission.

Additionally, CORTO has been applied in two ASI and ESA projects, notably DeepNav [24] and StarNav [25, 26]. For DeepNav, CORTO was used to generate training and testing datasets to design and implement deep learning techniques for visual-based navigation around small bodies using onboard accelerators. In the StarNav project, CORTO was employed to generate star tracker images to investigate image-processing capabilities for operations around the Moon and small bodies.

Beyond these projects, CORTO can generate a variety of image-label pairs for different operational scenarios, ranging from small body exploration and planetary exploration to imaging artificial bodies. The next section will further explore these aspects to demonstrate the tool capabilities.

3.1 Small Bodies

CORTO was originally designed for small-body close-proximity operations due to the limited data available from previous missions to these bodies. The tool aimed to address the need for extensive datasets to validate and test image processing and visual-based navigation pipelines. Consequently, many of its current functionalities are tailored specifically for this case study.

Currently, CORTO can simulate small-body scenarios across all mission phases, from distant approaches to close-proximity operations.
Small bodies can be rendered with available textures or a variety of reflectivity models, including Lommel-Seeliger [27], ROLO [28], Akimov [29, 30], Linear Akimov [31], Lunar Lambert [32], and Minnaert [33]. An example of this is the rendering of the Didymos binary system shown in Figure 2. Additionally, the tool supports the procedural generation of shapes and key morphological characteristics, such as roughness, craters, and boulders, using the Minor bOdy geNErator Tool (MONET). This capability enables the creation of a vast array of surface features to test the robustness of navigation algorithms under extreme conditions. A mosaic of minor bodies showcasing MONET capabilities is illustrated in Figure 3.

The true power of CORTO lies in its ability to generate extensive amounts of labels for various applications, such as instance segmentation, body recognition, pose estimation, and hazard detection. Key labels that can be generated for orbiting minor bodies include segmented images distinguishing boulders, surface, and background, slope maps, height maps, and crater detection.

3.2 Planetary

Planetary applications have also been explored, including far-relative optical navigation for the Moon, Mars, and Earth, with plans for future bodies as well. Surface exploration has been investigated and will be integrated into the tool in the future.

3.2.1 Far range (Moon)

The Moon has been used as a case study for limb-based relative navigation and crater detection algorithms. The latter case is exemplified by Figure 4, which shows craters labels generated using the high-fidelity texture map obtained by the Robbins [34] crater dataset [9].

3.2.2 Surface exploration (Mars)

The successful demonstration flights of the NASA's Mars Helicopter, Ingenuity, marked a transformative step in the surface exploration and scientific discovery on Mars, by introducing the aerial mobility dimension [35]. Future Mars rotorcrafts, such as the Mars Science Helicopter (MSH), will require even more advanced autonomous navigation capabilities to access diverse terrains and perform long-range, fully autonomous flights, aiming to enable high-priority investigations in astrobiology, climate, and

[9] https://astrogeology.usgs.gov/search/map/Moon/Research/Craters/lunar_crater_database_robbins_2018, last accessed 10th of September, 2024.

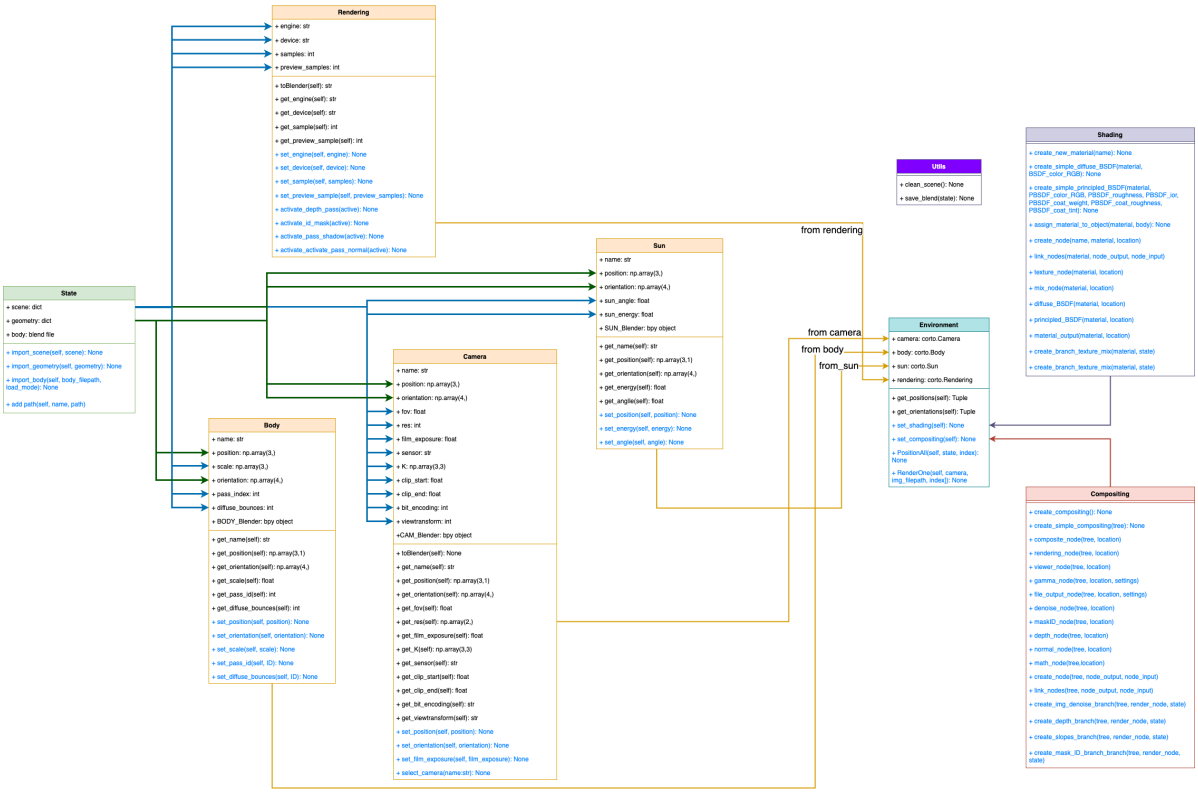

Fig. 1: UML diagram of the CORTO architecture

Fig. 2: Example of a rendering of Didymos and Dimorphos used in [22].

geology on Mars [36, 37]. The generation of synthetic datasets depicting Martian terrain will play a pivotal role in developing and validating these capabilities, ensuring robustness across diverse environmental conditions and mission scenarios. A meaningful application is the use of synthetic Mars image datasets to validate map-based localization pipelines. To achieve precision during long-range traverses on complex terrains, it's essential to minimize drift in position estimates generated by on-board visual odometry. This can be accomplished by registering images captured by the on-board navigation camera with pre-referenced orbital maps, such as those generated from the HiRISE camera aboard the Mars Reconnaissance Orbiter. However, previous studies have demonstrated that map-based localization is most affected when onboard images are captured under lighting conditions that differ from those of the reference orbital images, especially over high-relief terrain [38]. This discrepancy can lead to increased drift over time, potentially limiting flight duration or restricting operations to specific times of day. Synthetic images of Martian terrain rendered under varying lighting conditions offer a way to test and enhance the resilience of map-based localization algorithms in challenging environments. Figure 6 illustrates an example of Martian terrain rendered in Blender with different lighting conditions, using publicly available HiRISE data.

A labeled dataset can be effectively used also to test other critical tasks, like on-bard autonomous landing site detection and hazard avoidance landing on unknown terrains [39]. It would be particularly beneficial also for training and test Machine Learning models for segmentation and object-detection in such applications. These examples highlight how CORTO can be extended to integrate Martian terrain dataset generation, enabling more

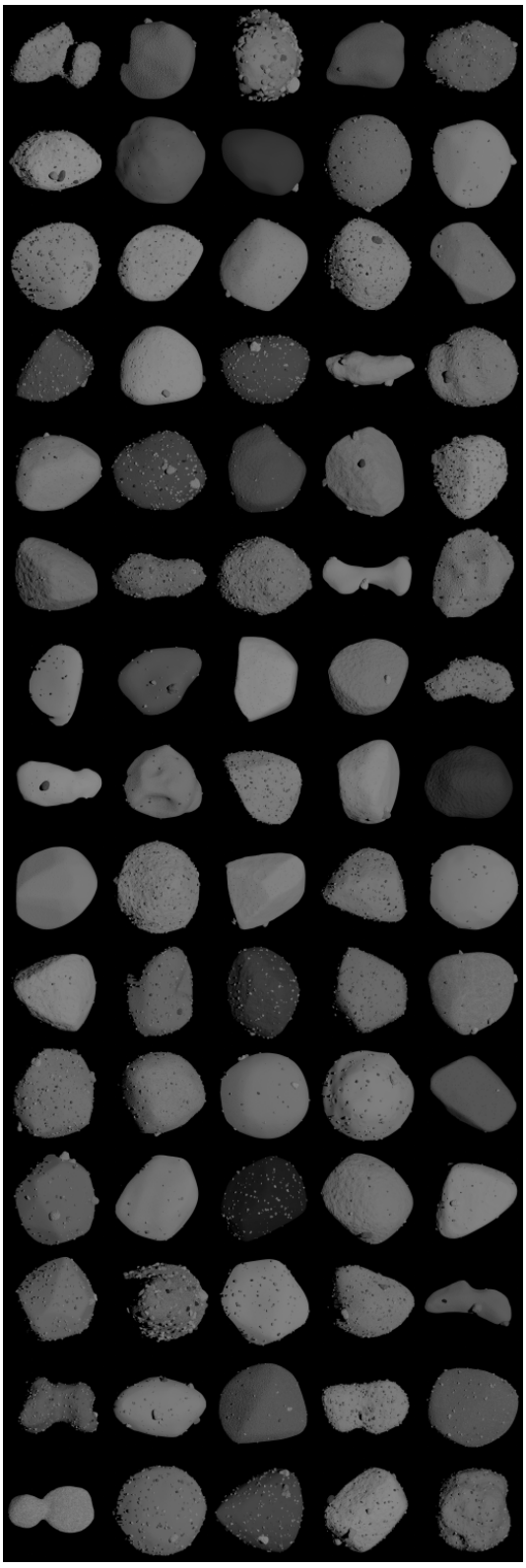

Fig. 3: Mosaic of 75 small bodies generated with MONET.

comprehensive simulations and validations across a wide range of operational scenarios. By incorporating diverse

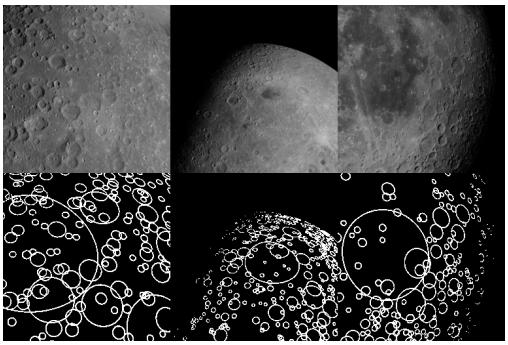

Fig. 4: Example of image-label pairs of the Moon surface with craters from the Robbin's dataset.

Fig. 5: Example of a synthetic rendering of the surface of the Moon for far navigation applications.

lighting conditions and realistic terrain features, CORTO will provide a robust framework for testing and refining autonomous visual-based navigation algorithms for Mars surface exploration tasks.

3.3 Artificial bodies

The capability of creating a general tool for the generation of synthetic images of artificial bodies has been gaining traction in recent years for specific application of relative navigation [40, 41, 42] dedicated to in-orbit servicing and active debris removal missions. In particular, these tasks benefit from the use of vision-based navigation algorithm due to the low power and mass budget of standard monocular cameras. The capability of generating realistic annotated datasets for training and validation of computer vision algorithms for proximity operations is therefore highly desirable [43], and it was preliminarily implemented in the JINS software [44]. This capability will also be ported to CORTO in a future release. In order to be used in the software, an artificial body model needs to be preprocessed. This step is a one-time-only procedure that starts with the subdivision of the Blender model into parts corresponding to the components of interest as

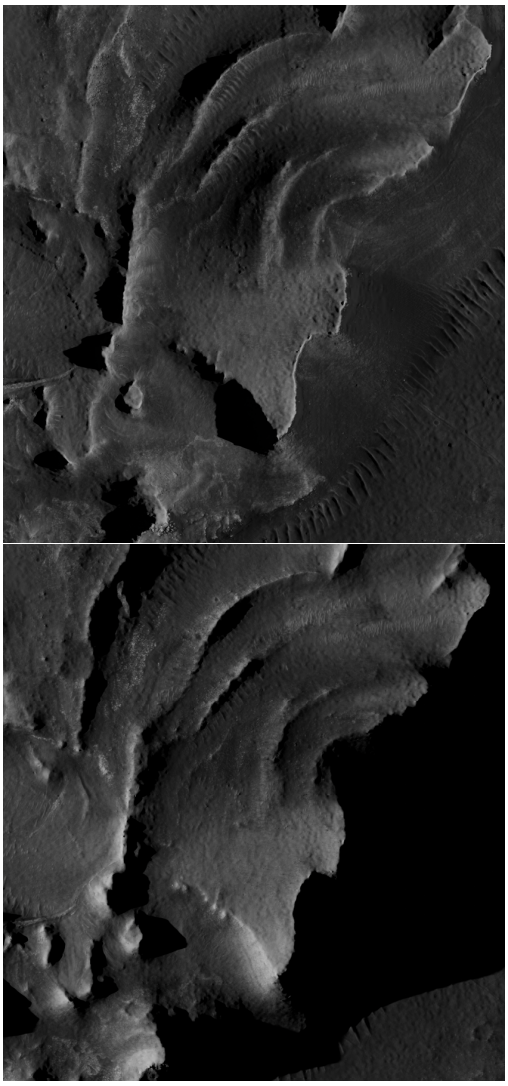

Fig. 6: Example of Martian terrain rendered in Blender under different illumination conditions.

Fig. 7: Example of a rendered image and the related masks identifying the different components [44].

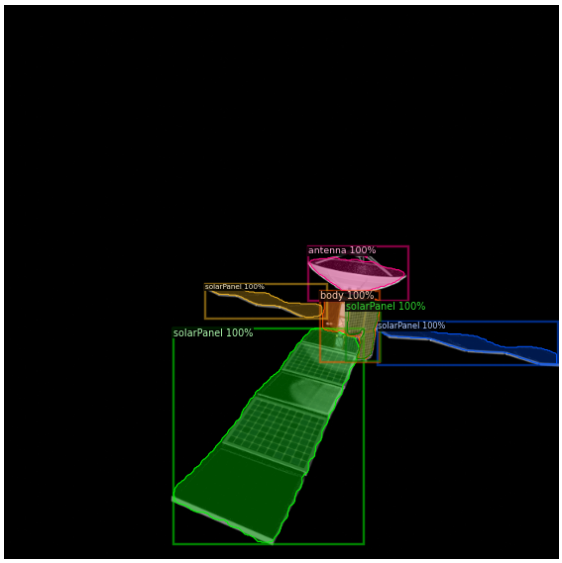

Fig. 8: Results from the inference on the single satellite datasets [44].

illustrated in Fig. 7

Each occurrence of these components included in the list of classes to be identified must be interpreted by the software as a distinct standalone object. Then, a custom property (i.e., object pass index) has to be specified for each of the parts of interest. Once the object is preprocessed and loaded into CORTO, it is possible to generate synthetic datasets of the object including information concerning pose, object detection, and instance segmentation for various spacecraft components (for further details see [45, 46]. The dataset generated with this approach can be used for inference on images of known objects as in Fig. 8 and unknown real objects (regardless of the training dataset) as illustrated in Fig. 9.

4. Tutorials walkthroughs

To run the repository two parts are needed: the *codebase* and the *data* folder. The *codebase* can be downloaded in two ways:

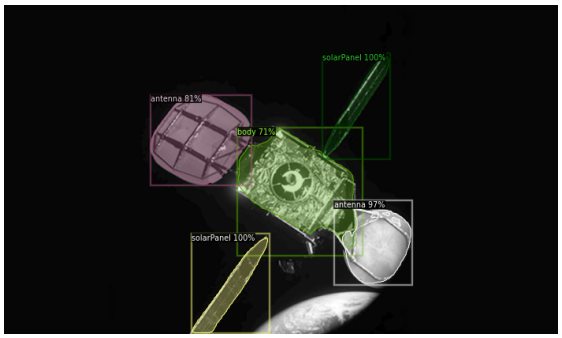

Fig. 9: Results from the inference on MEV-1 real images [44].

cloning

```
git clone https://github.com/MattiaPugliatti/corto.git
```

or

pip

```
pip install cortopy
```

The *data* folder has to be manually downloaded from `https://drive.google.com/drive/folders/1K3e5MyQin6T9d_EXLG_gFywJt3I18r6H?usp=sharing`. The data folder only contains dedicated data to run the tutorial, and needs to be located at the same level of the corto directory. The user can mimick this structure to position its own sets of input.

To run a tutorial, just download both the *codebase* and *data* folders of the desired scenario and run the corresponding script within the */tutorial* path of the repository:

- **demo_S01_Eros.py** Single asteroid case with Eros. Textured body. Depth and slope maps as labels.
- **demo_S02_Itokawa.py** Single asteroid case with Itokawa. Textured body. Depth and slope maps as labels.
- **demo_S03_Bennu.py** Single asteroid case with Bennu. Textured body. Depth and slope maps as labels.
- **demo_S04_Didymos.py** Binary asteroid case with Didymos, shape models after DART impact. Procedurally generated surface. Depth and slope maps, ID masks with and without shadows as labels.
- **demo_S05_Didymos_Milani.py** Binary asteroid case with Didymos, shape models before DART impact. Procedurally generated surface. Blend model used for the design of the IP of Milani. Depth and slope maps, and object ID masks with and without shadows as labels.
- **demo_S06_Moon.py** Planetary body case with the Moon. Textured body. Depth as label.

The tutorials are meant to showcase CORTO functionalities. The user can either use these case scenarios or adapt them to their needs.

5. Validation

5.1 Radiometric Calibration

CORTO has to be radiometrically calibrated to return the true energy content of an image, considering the properties of the camera that is being used. In fact, the brightness of the image depends on pupil size, quantum efficiency, transmissivity, exposure time, and other parameters that are not explicitly settable in Blender but shall be embedded in the value of the Solar Strength of the light node through a radiometric calibration procedure.

The calibration involves the rendering of a simple 1-meter radius Lambertian sphere and the comparison of the number of electrons collected by each pixel against a ground-truth radiometric model [47]. An example is depicted in Figure 10. The calibration is complete when the scatter plot aligns with the red diagonal. After that, all the consequent renderings will return radiometric content that is consistent with the one that would be collected by the same camera in reality.

As for now, every time the light-dependant camera parameters change, the calibration has to be performed again.

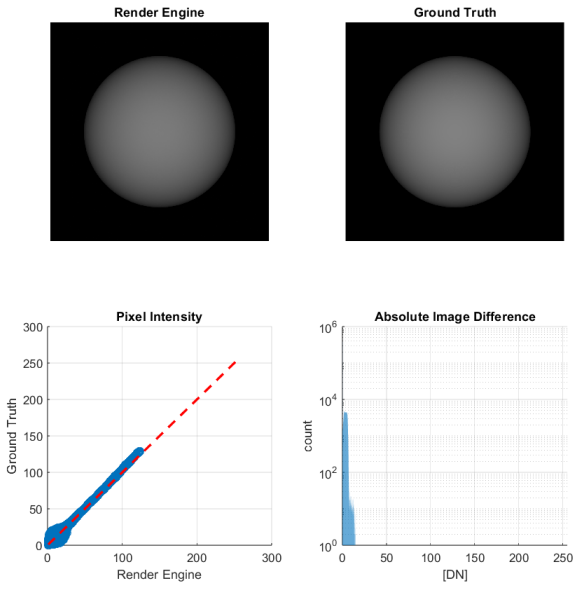

Fig. 10: Radiometric calibration.

5.2 End-to-End Comparison

To validate the calibration procedure, an end-to-end comparison of a Moon image has been performed against

real space imagery acquired with the AMIE camera of the SMART-1 mission. These images are available open-source with associated metadata[10], both in terms of radiometry (camera characteristics and exposure time) and geometry (SPICE kernels). Consequently, after calibration against AMIE camera characteristics, the scene can be rendered in CORTO by converting the SMART-1 state to the Blender reference frame. An example of a picture taken during the Earth Escape trajectory on 19th August 2004 at 30 ms exposure[11] is shown in Figure 11. An Oren-Nayar model [48] with 0.3 roughness has been used as shader in Blender. After alignment of the frames through normalized cross-correlation and removal of the background noise from the real image, a quantitative analysis has been performed through the Structural Similarity Index Measure (SSIM). As it can be seen in Figure 12, the SSIM reveals metrics of 0.99, 0.99 and 0.98 on Luminance, Contrast and Structure. This can be considered a good result for a preliminary validation, accounting for the fact that distortions, diffraction and noise effects have not been applied to the rendered image and more accurate reflection models (e.g. Hapke) have not been used. A small geometry mismatch for limb and terminator is in any case expected to be present since knowledge of ephemeris is affected by uncertainties [49].

Fig. 11: Real AMIE image (left) vs CORTO rendering (right)

Fig. 12: Quantitative assessment of similarity using SSIM.

6. Conclusions

This work showcased CORTO, a collaborative, modular, python library that can be used to synthetically generate a variety of image-label pairs. CORTO has been designed to encourage collaboration between experts in the field from different sectors, decreasing the burden associated to dataset generation and unlocking new opportunities for the design and testing of image processing algorithms.

CORTO is currently in v1.0. Future works will focus on expanding the set of scenarios that can be simulated, adding valuable pipelines for dataset generation, and designing an automatic calibration procedure at the script level that does not require intervention from the user.

[10] AMIE Image Database. Last accessed 10th of September, 2024.
[11] AMI_EE3_040819_00208_00030.IMG

References

[1] Martin I, Dunstan M, Gestido MS. Planetary surface image generation for testing future space missions with pangu. In *2nd RPI Space Imaging Workshop*, 2019, 1–13.

[2] Martin I, Dunstan M. PANGU v6: Planet and Asteroid Natural Scene Generation Utility, 2021.

[3] Parkes S, Martin I, Dunstan M, Matthews D. Planet surface simulation with pangu. In *Space ops 2004 conference*, 2004, 389.

[4] Lebreton J, Brochard R, Baudry M, Jonniaux G, Salah AH, Kanani K, Goff ML, Masson A, Ollagnier N, Panicucci P, Proag A, Robin C. Image simulation for space applications with the SurRender software. In *11th International ESA Conference on Guidance, Navigation & Control Systems, 22 - 25 June*, 2021, 1–16.

[5] Brochard R, Lebreton J, Robin C, Kanani K, Jonniaux G, Masson A, Despré N, Berjaoui A. Scientific image rendering for space scenes with the SurRender software, 2018.

[6] Pajusalu M, Iakubivskyi I, Schwarzkopf GJ, Knuuttila O, Väisänen T, Bührer M, Palos MF, Teras H, Le Bonhomme G, Praks J, et al.. SISPO: Space Imaging Simulator for Proximity Operations. *PloS one*, 2022, 17(3): e0263882.

[7] Iakubivskyi I, Mačiulis L, Janhunen P, Dalbins J, Noorma M, Slavinskis A. Aspects of nanospacecraft design for main-belt sailing voyage. *Advances in Space Research*, 2021, 67(9): 2957–2980, doi:https://doi.org/10.1016/j.asr.2020.07.023, solar Sailing: Concepts, Technology, and Missions II.

[8] Snodgrass C, Jones GH. The European Space Agency's Comet Interceptor lies in wait. *Nature Communications*, 2019, 10(1), doi:10.1038/s41467-019-13470-1.

[9] Kenneally PW, Piggott S, Schaub H. Basilisk: A Flexible, Scalable and Modular Astrodynamics Simulation Framework. *Journal of Aerospace Information Systems*, 2020, 17(9): 496–507, doi:10.2514/1.i010762.

[10] Teil TF. Optical Navigation using Near Celestial Bodies for Spacecraft Autonomy. Ph.D. thesis, University of Colorado at Boulder, 2020.

[11] Teil T, Schaub H, Kubitschek D. Centroid and Apparent Diameter Optical Navigation on Mars Orbit. *Journal of Spacecraft and Rockets*, 2021, 58(4): 1107–1119, doi:10.2514/1.a34815.

[12] Teil T, Bateman S, Schaub H. Autonomous On-orbit Optical Navigation Techniques For Robust Pose-Estimation. *Advances in the Astronautical Sciences AAS Guidance, Navigation, and Control*, 2020, 172.

[13] Teil T, Bateman S, Schaub H. Closed-Loop Software Architecture for Spacecraft Optical Navigation and Control Development. *The Journal of the Astronautical Sciences*, 2020, 67: 1575–1599.

[14] Villa J, Bandyopadhyay S, Morrell B, Hockman B, Bhaskaran S, Nesnas I, et al.. Optical navigation for autonomous approach of small unknown bodies. In *43rd Annual AAS Guidance, Navigation & Control Conference*, volume 30, 2019, 1–3.

[15] Villa J, Mcmahon J, Nesnas I. Image Rendering and Terrain Generation of Planetary Surfaces Using Source-Available Tools. In *46th Annual AAS Guidance, Navigation & Control Conference*, 2023, 1–24.

[16] Peñarroya P, Centuori S, Hermosín P. AstroSim: A GNC simulation tool for small body environments. In *AIAA SCITECH 2022 Forum*, 2022, 2355.

[17] Lopez AE, Ghiglino P, Sanjurjo-rivo M. Churinet - Applying Deep Learning for Minor Bodies Optical Navigation. *IEEE Transactions on Aerospace and Electronic Systems*, 2022: 1–14, doi:10.1109/TAES.2022.3227497.

[18] Bhaskara R, Georgakis G, Nash J, Cameron M, Bowkett J, Ansar A, Majji M, Backes P. Icy Moon Surface Simulation and Stereo Depth Estimation for Sampling Autonomy. *IEEE Aerospace Conference*, 2024.

[19] Hough K, Mohammadi ME, Owens C, Bloom M, Moon L, Lincoln T, Horchler AD. DEMkit & LunaRay: Tools for Mission Data Generation and Validation. In *3rd Space Imaging Workshop*, 2022.

[20] Pugliatti M, Buonagura C, Topputo F. CORTO: The Celestial Object Rendering TOol at DART Lab. *Sensors*, 2023, 23(23): 9595, doi:10.3390/s23239595.

[21] Buonagura C, Pugliatti M, Topputo F. MONET: The Minor Body Generator Tool at DART Lab. *Sensors*, 2024, 24(11): 3658, doi:10.3390/s24113658.

[22] Pugliatti M, Piccolo F, Rizza A, Franzese V, Topputo F. The vision-based guidance, navigation, and control system of Hera's Milani Cubesat. *Acta Astronautica*, 2023, 210: 14–28, doi:10.1016/j.actaastro.2023.04.047.

[23] Topputo F, Merisio G, Franzese V, Giordano C, Massari M, Pilato G, Labate D, Cervone A, Speretta S, Menicucci A, Turan E, Bertels E, Vennekens J, Walker R, Koschny D. Meteoroids detection with the LUMIO lunar CubeSat. *Icarus*, 2023, 389: 115213, doi:https://doi.org/10.1016/j.icarus.2022.115213.

[24] Buonagura C, Pugliatti M, Franzese V, Topputo F, Zeqaj A, Zannoni M, Varile M, Bloise I, Fontana F, Rossi F, et al.. Deep Learning for Navigation of Small Satellites About Asteroids: An Introduction to the DeepNav Project. In *International Conference on Applied Intelligence and Informatics*, Springer, 259–271.

[25] Piccolo F, Balossi C, Panicucci P, Pugliatti M, Topputo F, Capolupo F. Resource-Constrained Vision-Based Relative Navigation About Small Bodies. In *46th AAS Guidance, Navigation and Control Conference, Breckenridge, Colorado*, 2024, 1–18.

[26] Balossi C, Piccolo F, Panicucci P, Pugliatti M, Topputo F, Capolupo F. Moon Limb-Based Autonomous Optical Navigation Using Star Trackers. In *46th AAS Guidance, Navigation and Control Conference, Breckenridge, Colorado*, 2024, 1–19.

[27] Seeliger H. Zur photometrie des saturnringes. *Astronomische Nachrichten*, 1884, 109: 305.

[28] Buratti B, Hicks M, Nettles J, Staid M, Pieters C, Sunshine J, Boardman J, Stone T. A wavelength-dependent visible and infrared spectrophotometric function for the Moon based on ROLO data. *Journal of Geophysical Research*, 2011, 116(E6), doi:10.1029/2010JE003724.

[29] Akimov LA. Influence of mesorelief on the brightness distribution over a planetary disk. *Soviet Astronomy*, 1975, 19: 385.

[30] Akimov LA. On the brightness distributions over the lunar and planetary disks. *Astronomicheskii Zhurnal*, 1979, 56: 412.

[31] Golish D, DellaGiustina D, Li JY, Clark B, Zou XD, Smith P, Rizos J, Hasselmann P, Bennett C, Fornasier S, et al.. Disk-resolved photometric modeling and properties of asteroid (101955) Bennu. *Icarus*, 2021, 357: 113724, doi:10.1016/j.icarus.2020.113724.

[32] McEwen AS. Photometric functions for photoclinometry and other applications. *Icarus*, 1991, 92(2): 298–311, doi:10.1016/0019-1035(91)90053-V.

[33] Minnaert M. The reciprocity principle in lunar photometry. *Astrophysical Journal*, 1941, 93: 403–410, doi:10.1086/144279.

[34] Robbins SJ. A new global database of lunar impact craters> 1–2 km: 1. Crater locations and sizes, comparisons with published databases, and global analysis. *Journal of Geophysical Research: Planets*, 2019, 124(4): 871–892.

[35] Grip HF, Conway D, Lam J, Williams N, Golombek MP, Brockers R, Mischna M, Cacan MR. Flying a Helicopter on Mars: How Ingenuity's Flights were Planned, Executed, and Analyzed. In *2022 IEEE Aerospace Conference (AERO)*, 2022, 1–17, doi:10.1109/AERO53065.2022.9843813.

[36] Bapst J, Parker TJ, Balaram J, Tzanetos T, Matthies LH, Edwards CD, Freeman A, Withrow-Maser S, Johnson W, Amador-French E, Bishop JL, Daubar IJ, Dundas CM, Fraeman AA, Hamilton CW, Hardgrove C, Horgan B, Leung CW, Lin Y, Mittelholz A, Weiss BP. Mars Science Helicopter: Compelling Science Enabled by an Aerial Platform. *Bulletin of the AAS*, 2021, 53(4), https://baas.aas.org/pub/2021n4i361.

[37] Tzanetos T, Bapst J, Kubiak G, Tosi LP, Sirlin S, Brockers R, Delaune J, Grip HF, Matthies L, Balaram J, Withrow-Maser S, Johnson W, Young L, Pipenberg B. Future of Mars Rotorcraft - Mars Science Helicopter. In *2022 IEEE Aerospace Conference (AERO)*, 2022, 1–16, doi:10.1109/AERO53065.2022.9843501.

[38] Brockers R, Proença P, Delaune J, Todd J, Matthies L, Tzanetos T, Balaram JB. On-board Absolute Localization Based on Orbital Imagery for a Future Mars Science Helicopter. In *2022 IEEE Aerospace Conference (AERO)*, 2022, 1–11, doi:10.1109/AERO53065.2022.9843673.

[39] Proença PF, Delaune J, Brockers R. Optimizing Terrain Mapping and Landing Site Detection for Autonomous UAVs, 2022.

[40] Maestrini M, De Luca MA, Di Lizia P. Relative Navigation Strategy About Unknown and Uncooperative Targets. *Journal of Guidance, Control, and Dynamics*, 2023, 46(9): 1708 – 1725, doi:10.2514/1.G007337.

[41] Maestrini M, Di Lizia P. COMBINA: Relative Navigation for Unknown Uncooperative Resident Space Object. In *AIAA Science and Technology Forum and Exposition, AIAA SciTech Forum 2022*, 2022, doi:10.2514/6.2022-2384, Paper No. AIAA 2022-2384.

[42] Kaidanovic D, Piazza M, Maestrini M, Di Lizia P. Deep learning-based relative navigation about uncooperative space objects. In *Proceedings of the 73rd International Astronautical Congress, 18-22 September, 2022, Paris, France.*, volume 2022-September, IAF, Paper No. IAC-22.C1.IPB.38.x70501.

[43] Razgus B, Maestrini M, Di Lizia P. Initial Attitude Acquisition for Uncooperative Resident Space Objects Using Principal Lines. In *AIAA SciTech Forum and Exposition, 2024*, 2024, doi:10.2514/6.2024-0201, Paper No. AIAA 2024-0201.

[44] Faraco N, Maestrini M, Di Lizia P. Instance segmentation for feature recognition on noncooperative resident space objects. *Journal of Spacecraft and Rockets*, 2022, 59(6): 2160–2174, doi:10.2514/1.A35260.

[45] Pugliatti M, Maestrini M. A multi-scale labeled dataset for boulder segmentation and navigation on small bodies. In *Proceedings of the 74th International Astronautical Congress, 02-06 October, 2023, Baku, Azerbaijan.*, volume 2023-October, IAF, Paper No. IAC-23,A3,4A,8,x78927.

[46] Pugliatti M, Maestrini M. Small-Body Segmentation Based on Morphological Features with a U-Shaped Network Architecture. *Journal of Spacecraft and Rockets*, 2022, 59(6): 1821 – 1835, doi:10.2514/1.A35447.

[47] Pizzetti A, Panicucci P, Topputo F. A Radiometric Consistent Render Procedure for Planets and Moons. *4th Space Imaging Workshop*, 2024: 1–3.

[48] Oren M, Nayar SK. Generalization of Lambert's reflectance model. *Proceedings of the 21st annual conference on Computer graphics and interactive techniques*, 1994, doi:10.1145/192161.192213.

[49] Belgacem I, Jonniaux G, Schmidt F. Image processing for precise geometry determination. *Planetary and Space Science*, 2020, 193: 105081, doi:https://doi.org/10.1016/j.pss.2020.105081.